46th AIAA Aerospace Sciences Meeting and Exhibit
7 - 10 January 2008, Reno, Nevada

AIAA 2008-134

Multi-Stage Aerodynamic Design of Multi-Body Geometries via Global and Local Optimization Methods

JinWoo Yim*, Byung Joon Lee†, and Chongam Kim.‡
School of Mechanical & Aerospace Eng., Seoul National Univ., Seoul, Korea, 151-742

Shigeru Obayashi§
Department of Aeronautic and Space Engineering, Tohoku Univ. Sendai, Japan

An efficient and high-fidelity design approach is proposed by combining global and local optimization methods for wing planform and surface design. For enhanced design results, aerodynamic shape optimization process is carried out via 2-stage with different optimization strategy. In the first stage, global optimization techniques are applied to planform design with a few geometric design variables. In the second stage, local optimization techniques are used for wing surface design with a lot of design variables to maintain a sufficient design space with high DOF (Degree of Freedom) geometric change. For global optimization, meta-modeling techniques such as RS (Response Surface) and Kriging methods are used in conjunction with Genetic Algorithm (GA). For local optimization, a discrete adjoint variable method is used. By the successive combination of global and local optimization techniques, drag minimization is performed for a multi-body aircraft configuration while maintaining the baseline lift and the wing weight at the same time. Through the design process, performances of the test models are remarkably improved in comparison with the single stage design approach. The capability of proposed design framework including wing planform design variables can be evaluated by the drag decomposition method which can provide improvement of induced drag and wave drag, respectively.

Nomenclature

b	=	span
C_D	=	drag coefficient $\left(= Drag/q_\infty S_{ref}\right)$
C_L	=	lift coefficient $\left(= Lift/q_\infty S_{ref}\right)$
c	=	chord length
Dv	=	design variables including mesh perturbation, span, sweepback and Mach number, and so on.
F	=	objective function (cost function) for design problem
q_∞	=	dynamic pressure based on free-stream condition $\left(= 1/2\rho_\infty V_\infty^2\right)$
S_{ref}	=	wing reference area
θ	=	twist angle along the spanwise direction

* Ph. D. Student (School of Mechanical & Aerospace Eng., Seoul National Univ., Korea), AIAA Student Member.
† Post Doc. (School of Mechanical & Aerospace Eng., Seoul National Univ., Korea), AIAA Member.
‡ Associate Professor (School of Mechanical & Aerospace Eng., Seoul National Univ., Korea), AIAA Senior Member and Corresponding Author, E-mail: chongam@snu.ac.kr
§ Professor (Department of Aeronautic and Space Engineering, Tohoku Univ., Sendai, Japan), AIAA Member

I. Introduction

AERODYNAMIC shape optimization becomes more and more popular in aircraft design field though flow physics shows a strong nonlinear characteristic. The strong nonlinearity makes it difficult to develop an accurate flow solver and it is time-consuming to obtain an accurate flow solution. At the same time, it affects the overall design process. If shape design variables such as wing section thickness and span are deformed a little from the baseline model, flow phenomenon around aircraft geometry is changed remarkably. However, because of this property, if design variables are controlled properly, aerodynamic performance can be increased efficiently. Various design optimization techniques have been developed and/or exploited to improve aerodynamic performance of aircraft. The design methodology can be usually classified into global and local optimization strategies according to the method of finding optimal values in design space. Each optimization method has its own merits and demerits depending on design problems.

Global optimization method may provide the global optimum value within the specified design space. For example, Genetic Algorithm(GA) originated from the theory of natural evolution is widely used as a global optimization tool[3,4,5] However, this method is generally costly in imitating an accurate evolutional process, and especially for three-dimensional aerodynamic design problems with a lot of design variables, it requires an enormous amount of computational time in evaluating experimental data at each deign point. For that reason, researches using GA as an aerodynamic shape optimization tool has a limitation that it is generally applied to problems with relatively small design variables. Therefore, approximation technique called meta-modeling that is originated from statistics is popularly adopted, such as RSM[2, 6] or Kriging[7, 8]. Once a meta-modeling is constructed by suitable mathematical function and experimental points in design space, it can predict new values immediately without any flow analysis. However, these modeling methods may also require a huge computational cost to obtain experimental data for building up the response model, if geometric shape is complex or the number of design variable is large. Furthermore, if sample experimental points representing objective function values in a complex design space are not appropriate, design results can be poorer than other optimization tools.

On the other hand, Gradient Based Optimization Method (GBOM) is also popularly used because computational cost of the adjoint approach is independent of the number of design variable[9-13] In addition, it exhibits a good convergence characteristic because GBOM uses the gradient vector of the objective function which provides an optimal direction in design space. Thus, it is particularly powerful in case of wing surface design which usually requires a lot of design variables. Jameson *et al.*[9] proposed continuous adjoint approach and applied it to aerodynamic shape optimization problems of several wing/body geometries with wing planform and surface design variables. Lee *et al.* extended the discrete adjoint method to overset mesh system, which can be applied to complex geometries with relatively simple grid topology.[10] Mavriplis [11], Nielsen [12], Kim [13] *et al.* also used the discrete adjoint method in design problems of various complex geometries on unstructured mesh systems. Through these applications, continuous or discrete adjoint variable methods have been demonstrated the capability to yield a substantial improvement of aerodynamic performance. However, despite the superior performance in transonic aerodynamic design problems, GBOM still has a potential danger to be trapped in local optimum during design process, especially in cases of noisy design spaces.

In the present study, an efficient multi-stage design strategy is proposed which takes advantages of both global and local optimization methods. Wing planform design which can be represented with a few design variables is performed by global optimization method using meta-modeling and GA optimizer. On the other hand, wing surface design which requires a lot of design variables for the sophisticated treatment of surface geometry is performed by the GBOM using the discrete adjoint approach. Finally, capability of the proposed multi-stage design approach including wing planform design variables is evaluated by carefully comparing drag reduction depending on design variables with drag decomposition method based on far-field analysis[14-17].

II. Numerical Methods

A. Meta-Modeling

Meta-modeling technique is commonly used to create approximation of the mean and variation of response in noisy design space, because its implementation is very simple. A meta-model is adopted as a surrogate approximation for actual experimental data or numerical analysis during the design process. Among the meta-modeling techniques, Response Surface Methodology (RSM) and Kriging model are the most popular techniques for aerodynamic shape design. RSM was originally developed to analyze experimental data and to create empirical models of the observed response values. The particular merit of RSM is its applicability to investigate a problem which only a few observations are available. For the sake of easy implementation, RSM commonly employs a

simple polynomial functions like Eq.(1) using the least square regression technique. However, accuracy of RSM is somewhat limited if physical phenomena are highly non-linear or noisy with respect to design variables.

$$y(x) = f(x) + \varepsilon . \tag{1}$$

Here, the function $y(x)$ is a response surface in the real design space with respect to the design variable *x*, and $f(x)$ is a polynomial function for the regression. ε denotes the error between the regression function and the real design space. This term may indicate a discrepancy between the predicted value from the response surface and the real performance of the designed geometry from a CFD solver.

In order to overcome this limitation, aerodynamic designers began to adopt a new meta-modeling technique, so called the Kriging method. The Kriging method was developed in the field of geostatistics, and it is useful in predicting temporally and spatially correlated data. Unlike the RSM, Kriging model can interpolate sample data exactly, and represent a function with multiple local extrema. As in Eq. (2), the Kriging modeling technique is composed of two elements.

$$y(x) = f(x) + Z(x) , \tag{2}$$

where $f(x)$ is a global regression model such as RSM or usually a constant value. $Z(x)$ is the realization of stationary Gaussian random function to calibrate local deviation from the global model. Using this term, multiple local extrema can be represented in contrast with the RSM. Thus, if physical phenomena depending on design variables are highly nonlinear or noisy, the Kriging can be more suitable than the RSM in fitting the global design space. However, in order to predict a new design point from the Kriging model, it requires more computational cost than the RSM, because the Kriging model cannot provide an explicit function in terms of design variables and predicted values.

B. Genetic Algorithm

Genetic Algorithm (GA) is a class of stochastic algorithm inspired by natural evolution, and has been applied to find optimum values in various fields. Starting with a randomly generated population of chromosomes, a GA carries out a process of fitness based selection and recombination to produce successor population or the next generation. During recombination, parent chromosomes are selected and their genetic material is recombined to generate the child generation. As this process is progressed iteratively, a sequence of successive generations evolves and average fitness of the chromosomes tends to increase until stopping criterion is reached. In this way, a GA evolves a best solution to a given design problem. An advantage of GA is that, unlike other optimization algorithms, it does not need gradient information. Therefore, if there are many local extrema and discontinuous properties, GA is more suitable in finding the global optimization point and design variable set than gradient based optimization methods. On the other hand, a GA requires substantial computational cost because of a large number of function evaluations. For that reason, there is a limit in the maximum number of design variable, and it may be prohibitive to apply the GA to complex aerodynamic shape optimization directly.

C. Discrete Adjoint Approach

If design space contains local extrema and discontinuities, non-gradient optimization methods such as GA are more suitable to find optimum values. On the other hand, if design space is relatively smooth and continuous, gradient based methods are much more efficient because of a good convergence behavior. Especially, adjoint variable method is the most powerful technique among the gradient based methods, because computational cost to solve the adjoint equations is not essentially influenced by the number of design variable. This is particularly useful when there are a lot of design variables such as wing surface design problems. However, this method requires solutions of additional adjoint equations to obtain gradient information for each objective function.

Assuming that the residual converges to the sufficient level near zero value either for steady-state or unsteady computations, the discrete adjoint formulation can be derived by the fully converged discrete governing equation and the objective function. These equations are dependent on flow variables (*Q*), computational grid (*X*) and design variables (*D*). Each equation can be differentiated by chain rule with respect to variables *Q*, *X* and *D*. In the adjoint method, gradient of the objective function can be re-written by incorporating the differentiated residual equation as in Eq. (3).

$$\left\{\frac{dF}{dD}\right\}=\left\{\frac{\partial F}{\partial Q}\right\}^{T}\left\{\frac{dQ}{dD}\right\}+\left\{\frac{\partial F}{\partial X}\right\}^{T}\left\{\frac{dX}{dD}\right\}+\left\{\frac{\partial F}{\partial D}\right\}+\Lambda^{T}\left(\left[\frac{\partial R}{\partial Q}\right]\left\{\frac{dQ}{dD}\right\}+\left[\frac{\partial R}{\partial X}\right]\left\{\frac{dX}{dD}\right\}+\left\{\frac{\partial R}{\partial D}\right\}\right). \quad (3)$$

Equation (3) can then be re-arranged into Eq. (4) to eliminate the {*dQ/dD*} term of which computational time cost increase in proportion to the number of design variable.

$$\left\{\frac{dF}{dD}\right\}=\left\{\frac{\partial F}{\partial X}\right\}^{T}\left\{\frac{dX}{dD}\right\}+\left\{\frac{\partial F}{\partial D}\right\}+\Lambda^{T}\left(\left[\frac{\partial R}{\partial X}\right]\left\{\frac{dX}{dD}\right\}+\left\{\frac{\partial R}{\partial D}\right\}\right)+\left(\left\{\frac{\partial F}{\partial Q}\right\}^{T}+\Lambda^{T}\left[\frac{\partial R}{\partial Q}\right]\right)\left\{\frac{dQ}{dD}\right\}. \quad (4)$$

If the adjoint vector Λ which makes the coefficient term of {*dQ/dD*} in Eq. (4) zero can be obtained through a time iterative method, sensitivity derivatives of the objective function can be directly calculated using Eq. (6).

$$\left\{\frac{\partial F}{\partial Q}\right\}^{T}+\Lambda^{T}\left[\frac{\partial R}{\partial Q}\right]=\{0\}^{T}, \quad (5)$$

$$\left\{\frac{dF}{dD}\right\}=\left\{\frac{\partial F}{\partial X}\right\}^{T}\left\{\frac{dX}{dD}\right\}+\left\{\frac{\partial F}{\partial D}\right\}+\Lambda^{T}\left(\left[\frac{\partial R}{\partial X}\right]\left\{\frac{dX}{dD}\right\}+\left\{\frac{\partial R}{\partial D}\right\}\right). \quad (6)$$

D. Drag Decomposition

The main goal of aerodynamic shape design is to minimize various components of drag, which may influence on the flight range of aircraft, overall fuel consumption, and/or structural constraints of the wing. For high-fidelity aerodynamic shape optimization, one of the most important issues is the accurate evaluation of aerodynamic performance. Many researchers made substantial efforts to accurately predict aerodynamic force by diminishing the discrepancy between numerically evaluated values and experimentally gauged data. One of the popular prediction methods is wake integration technique (or far-field method) originated from the momentum conservation theorem. [16-19] The drag prediction equation for wake integration can be given as follows. Equations (7) and (8) are derived by using small perturbation approximation.

$$D=\iint_{WA}P_{\infty}\frac{\Delta s}{R}ds+\iint_{WA}\frac{\rho_{\infty}}{2}(u^{2}+v^{2})ds+O(\Delta^{2}), \quad (7)$$

$$D_{Induced}=\iint_{WA}\frac{\rho_{\infty}}{2}(u^{2}+v^{2})ds\approx\iint_{WA}\frac{\rho_{\infty}}{2}\varphi\xi ds. \quad (8)$$

The first term on the right hand side of Eq. (7) represents entropy drag, and the second term is the induced drag. In case of the Euler flow analysis, the entropy drag consists of the wave drag and the spurious drag due to numerical dissipation. The second term is the induced drag originated from the vorticity generated by the wing tip. It can be expressed in terms of vorticity and stream function as in Eq. (8), to save computational cost and to give physically intuitive meaning.[15]

III. Design Optimization Framework

In order to obtain high-fidelity design results, design process of a wing can be organized by multiple stages according to goal of each design process as shown in Fig.1. In each design stage, optimization technique is essentially determined by the number of design variable and the degree of non-linearity of the design space. In case of wing planform design, the range of design variables is relatively wide in comparison with wing surface design. Therefore, a gradient based optimization method may be incapable of securing a sufficient performance even after design. It is because a design space which covers a wide range of design variables may contain non-linear

characteristics, and an optimal solution may be trapped in local optimal region. In addition, the number of design variable is at most about 4~6. Thus, global optimization method, which is time-consuming but capable of finding the optimal value even in non-linear design space, can be a good choice.

On the other hand, change of design variables is much smaller in wing surface design compared to planform design. Each design variable is not highly non-linear so that they can be represented by 2nd order polynomial functions in a localized design space as shown in Fig.2. Moreover, surface design requires a lot of design variables which excludes application of global optimization techniques to the design work. Thus, previous researches on the wing surface design commonly applied gradient based optimization method using an adjoint method. In these researches, they could obtain a shock-free wing successfully which may be a global optimum. In the present research, we also apply adjoint approach to the 2nd stage of wing surface design.

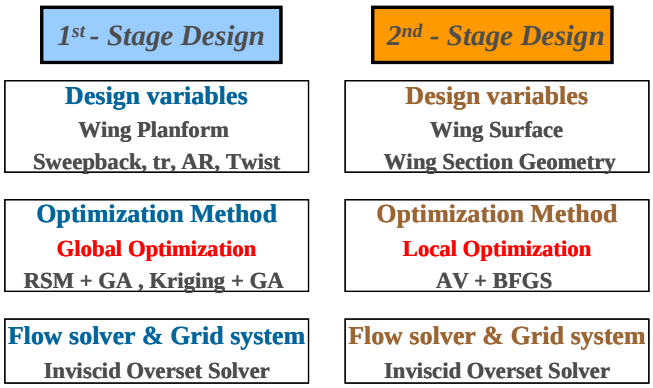

Figure 1. Strategy of 2-stage design.

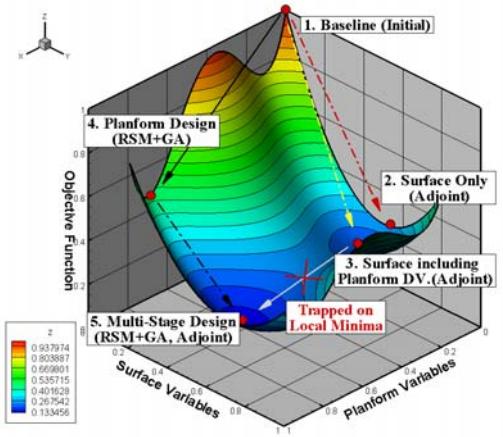

Figure 2. Schematic illustration of 2-stage design.

A schematic illustration of the present design framework in a drag minimization problem is given in Fig. 2. Design space is represented by a simple 3-dimensional function with respect to surface and planform design variables. From the baseline geometry at point 1, surface design process via GBOM may result in a design solution at point 2. The GBOM process including planform design variable can improve the design result from point 2 to point 3. However, the solution at point 3 may still remain at the local optimum. If we can acquire the global optimal solution (or a better solution) through planform design process as given by point 4, it is possible that the solution may reach point 5 passing through the local extremum between the points 3 and 5. If design space is highly non-linear in the direction of surface design variables, the point 5 would still be another local optimum. Even in such case, however, the present design framework can provide a best alternative to cure the limitation of the GBOM approach.

A. Planform Design using Global Optimization Approach

As shown in Fig.3, a wing planform can be represented by several design variables such as wing span, taper ratio, sweepback angle and twist angle. GA optimizer can be directly used for finding the global optimum values but this approach may require a prohibitive computational cost especially. Generally, GA needs thousands times of flow analyses for only a few design variables. In order to increase efficiency of the global optimization, a meta-model is firstly constructed using the RSM or Kriging model, and then GA is introduced to find the globally optimal geometry from the meta-model. Experimental data points are determined through Central-Composite Experimental Design (CCD) method based on Design of Experiment (DOE) theory, and the solution at each experimental point are evaluated by CFD solver. Using the evaluated experimental points, the meta-model can be

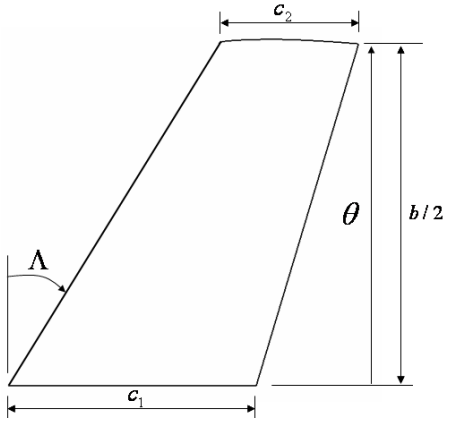

Figure 3. Planform variables of ONERA-M6.

constructed. Finally, GA optimizer is applied to find the globally optimal geometry with respect to the wing planform design variables. As a test case of the present multi-stage design approach, global optimization method is applied to the ONERA-M6 wing. Planform design variables are shown in Fig. 3 and Table 1. The objective of design process is the minimization of drag coefficient. Lift coefficient is maintained at the value of the baseline model during the design process as like Eq. (9).

$$\begin{aligned} &Minimize: C_D \\ &Subject\ to: C_L \geq C_{L_0}, C_{L_0} = (Lift\ coefficient\ of\ Baseline\ Model) \end{aligned} \tag{9}$$

The free stream Mach number is 0.84, and the angle of attack is 3.06 degree. The governing equations are the three-dimensional compressible Euler equations. For the spatial discretization, RoeM scheme[1] is used, and MUSCL(Monotonic Upstream Centered Scheme for Conservation Law) approach using a third order interpolation is applied for a higher order spatial accuracy. For time integration, LU-SGS scheme is applied.

Design variable(Dv)		Min	Baseline	Max	Opt. RSM	Opt. Kriging
Dv1	**Sweepback Angle** (Λ)	25°	30	35°	34.999	34.998
Dv2	**Half Span** $(b/2)$	1.3240	1.4712	1.6183	1.602008	1.536752
Dv3	**Taper Ratio** (c_2/c_1)	0.5058	0.562	0.6182	0.542367	0.549260
Dv4	**Twist Angle** (θ)	-2°	0	2°	0.137859	-0.000058

Table 1. Geometric information of ONERA-M6 and the designed wing.

Table 1 shows a set of planform variables for the optimal geometry. By comparing the results from RSM and Kriging model, most of the design variables show similar values except the twist angle. After obtaining the optimum values using meta-modeling and GA optimizer, predicted values and real values from CFD solver are compared to investigate the accuracy of meta-modeling and GA optimizer. Table 2 shows comparison of predicted values and real values. Predicted values are obtained by RSM and Kriging modeling with GA optimizer, and real values are evaluated by the flow solver using optimized design variables. In general, predicted values show a pretty good agreement with real values, which shows that the planform design tool works well. In this test case, the RSM yields slightly better results than the Kriging method.

Obj. fn. & Constraint	Baseline model	RSM		Kriging	
		Predicted value	Real value	Predicted value	Real value
C_L	0.261746	0.2617714	0.2618666	0.26174	0.2601053
C_D	0.011937	0.0102230	0.0101579	0.01059	0.0103969

Table 2. Comparison of objective functions/constraint values from planform design (planform design / ONEAR-M6).

Figures 4 and 6 depict the baseline and designed planforms from RSM and Kriging model. Figures 5 and 7 show pressure contours of the designed model for Kriging and RSM. Shock waves on upper wing surface are not remarkably weakened. It is because drag reduction effect during the planform design comes from both the reduction of induced drag and wave drag. Thus, drag decomposition method is adopted to identify the portion of induced drag reduction from the whole drag reduction as shown in Table.4 and the detailed analysis of the results will be given in chapter III-C.

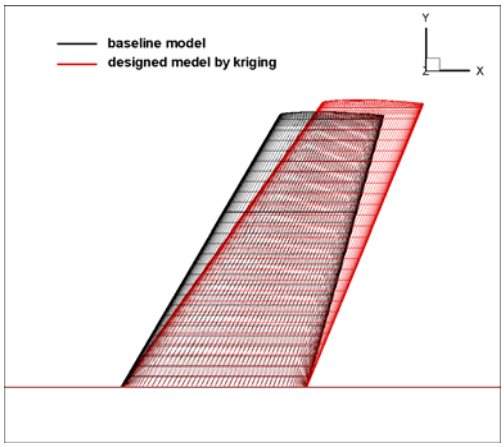

Figure 4. Comparison of baseline model with optimized model by Kriging method.

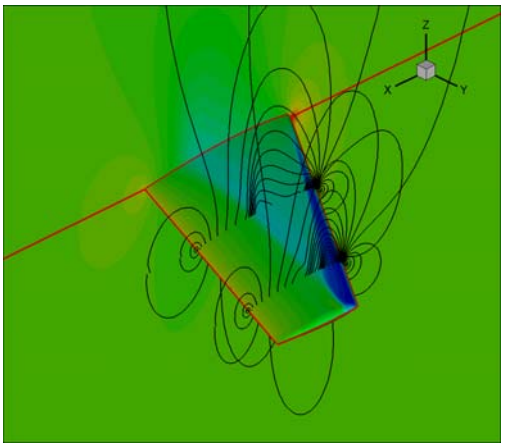

Figure 5. Pressure contour of the designed planform by Kriging method.

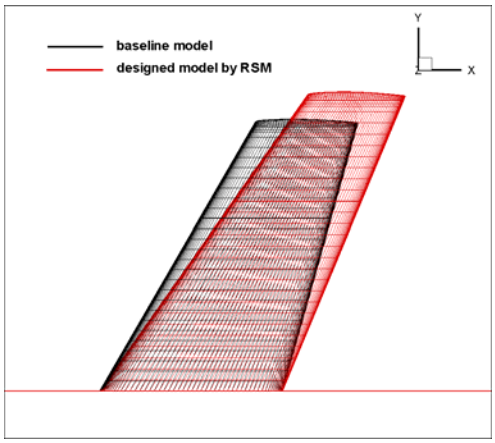

Figure 6. Comparison of baseline model with optimized model by RSM.

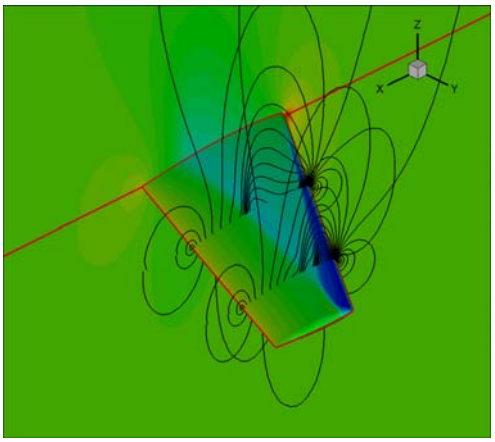

Figure 7. Pressure contour of the designed planform by RSM.

B. Surface Design using Local Optimization

Wing surface design is performed by using discrete adjoint approach to diminish wave drag. Since a large number of design variables are usually required to control change of wing surface geometry, adjoint approach is more appropriate than GA method even if it may be trapped in local optimum region. As shown in Fig. 8, three design sections are defined along the spanwise direction. 10 design variables are positioned at each design section of upper and lower surface respectively. Total 60 design variables are used in this case. Wing surface at each section is deformed by using Hicks-Henne functions. Design formulation is given by Eq. (10). In order to calibrate the variation of drag and lift coefficients, the weight factor for the lift constraint is given by the sensitivity ratio of drag to lift coefficient with respect to the angle of attack.

$$\begin{aligned} &Minimize : C_D \\ &Subject\ to : C_L \geq C_{L_0}, C_{L_0} = (Lift\ coefficient\ of\ Baseline\ Model) \\ &(Objective\ function) = C_D + Wt \times \left[0, C_{L_0} - C_L\right], \quad Wt = \frac{\partial C_D}{\partial \alpha} \Big/ \frac{\partial C_L}{\partial \alpha} \end{aligned} \tag{10}$$

Figure 9 shows surface design history. Drag coefficient decreases from 0.0119 to 0.0079(32% reduction) after 15 design iterations, while lift coefficient maintains at the initial value of 0.2600. In Figures 10 and 11, the shock strength on the wing surface decreases after surface design.

C. Multi-Stage Design

At the 1st stage design, the designed geometry by RSM yields a better performance than that by Kriging model as shown in Table 3. The lift constraint of the objective function in Eq. (10) behaves more favorably in RSM case. Thus, the 2nd stage design is performed with the planform designed by RSM and GA method. After 2-stage design, lift coefficient slightly decreases (0.7% reduction). On the other hand, drag coefficient considerably decreases from 0.011937 to 0.007262(39.2% reduction). Consequently, *L/D* is enhanced from 21.927 to 35.805(63.3% increase) as shown Figure 13, and the Λ shock on the upper wing surface is remarkably weakened in Figure 12.

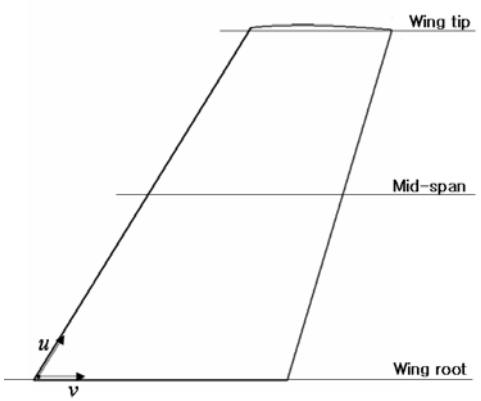

Figure 8. Surface variables (transonic wing design).

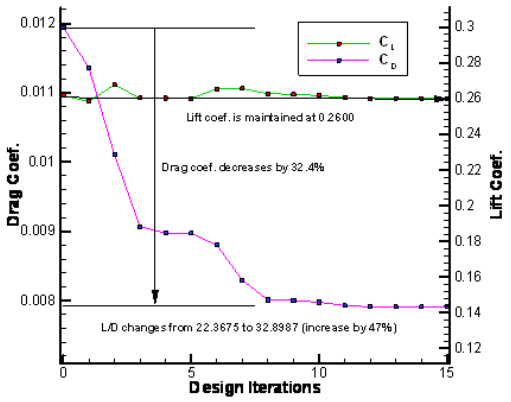

Figure 9. Deign history (transonic wing design).

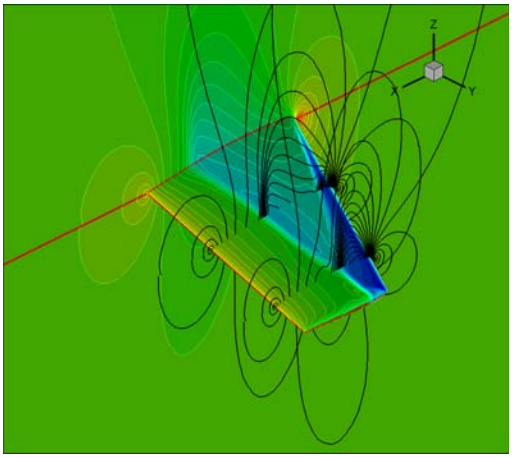

Figure 10. Pressure contour of baseline model.

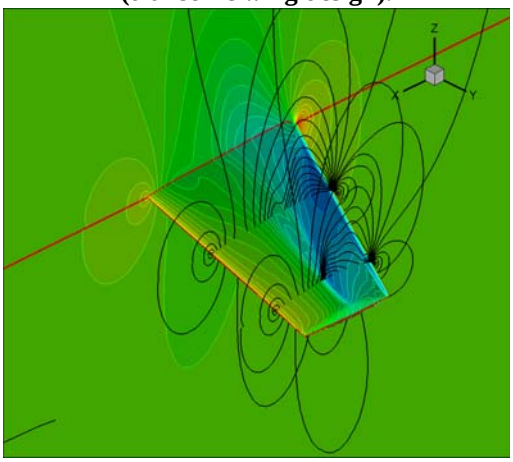

Figure 11. Pressure contour of surface designed model.

Obj. fn. & Constraint	Baseline model	Planform design only		Surface design Only (Adjoint)	Multi-stage design
		RSM + GA	Kriging + GA		RSM + Adjoint
C_L	0.261746	0.2618661	0.2601053	0.259997	0.260017
C_D	0.011937	0.0101579	0.0103969	0.007868	0.007262

Table 3. Comparison of objective functions/constraint values for designed models (ONERA-M6).

Drag coefficient is decomposed by using wake integration method (far-field method) to investigate the drag portion after wing planform and surface optimization in Table 4. In viscous flow, shock strength is relatively weak due to viscous effect. However, flow over wing upper surface is more accelerated in inviscid analysis, which induces a strong shock on wing surface. Thus, the amount of induced drag is not large compared with entropy drag when total drag of the baseline model is decomposed as shown in Table 4. For that reason, entropy drag reduction at every design step is larger than induced drag reduction, and entropy drag substantially decreases after surface design.

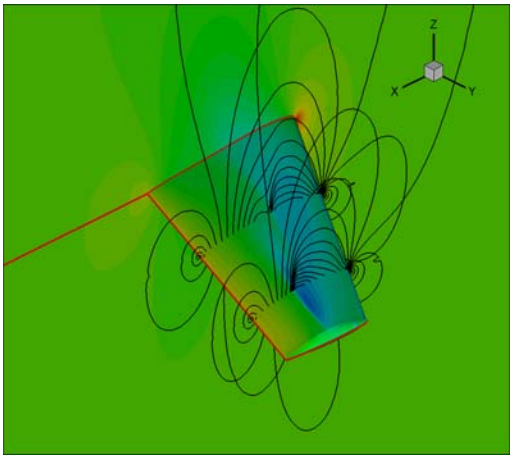

Figure 12. Pressure contour of 2-stage designed model.

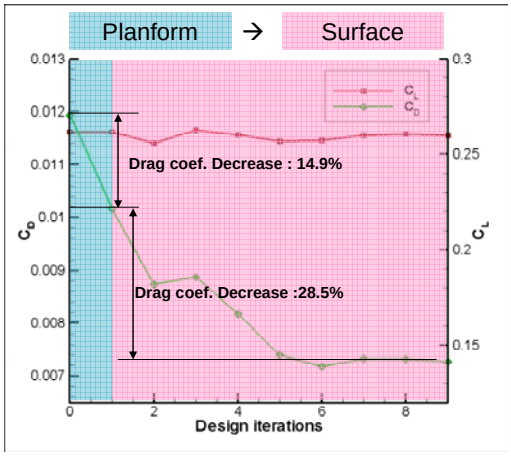

Figure 13. 2-stage design history of ONERA-M6.

Design strategy	Drag prediction method	C_L	C_D	C_D - entropy	C_D - induced
Baseline model	Surface integration	0.261746	0.011937	N/A	N/A
	Wake integration	0.267401	0.010837	0.00738432	0.00345286
Planform only (RSM + GA)	Surface integration	0.261789	0.010160	N/A	N/A
	Wake integration	0.273445	0.009546	0.00638865	0.00315782
Surface only (AV + BFGS)	Surface integration	0.263362	0.007868	N/A	N/A
	Wake integration	0.270641	0.007347	0.00360265	0.00374472
2-stage design	Surface integration	0.260017	0.007262	N/A	N/A
	Wake integration	0.273269	0.007413	0.00404691	0.00336635

Table 4. Comparison of aerodynamic performances evaluated by drag decomposition methods for the baseline and designed models.

IV. Multi-Stage Design Application

A. Definition of Design Problem

As an application of the present multi-stage design approach, a re-design problem of the DLR-F4 wing-body configuration is carried out. Planform design variables are similar to the case of the ONER-M6 wing. In order to provide physically acceptable design results, a wing weight constraint obtained by statistical group weight method[17] is incorporated at planform design step. The optimizer tends to increase the span to reduce induced drag, and decrease the thickness of wing section to reduce wave drag. Without the constraint of the wing weight, the designed wing may have severe problems in terms of structural safety and fuel storage. Figures 14 and 15 show design variables. Variables for planform design are span, chord length at the kink and wing tip position, sweep-back angle and twist angle. As shown in Figs. 15, 10, design sections are defined along the spanwise direction by considering large aspect ratio of the baseline wing. 10 design variables are positioned at each section of upper and lower surface, respectively. Total 200 design variables are used. Wing surface at each section is deformed using Hicks-Henne functions for smooth deformation. Regions between design sections are deformed by using linear interpolation.

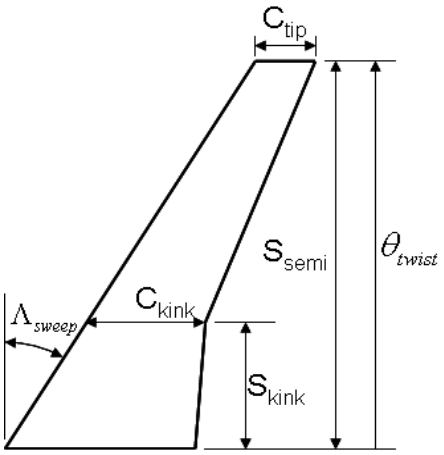

Figure 14. Wing planform variables of DLR-F4.

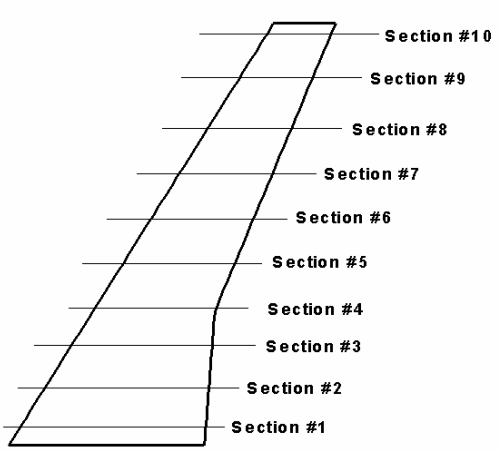

Figure 15. Surface variables of DLR-F4 wing.

In order to compute multi-body configuration, overset mesh system is used. Figure 16 shows the overall mesh system composed of 7 blocks: a global box ($77\times38\times72$), a fuselage box($84\times26\times45$), a wing box($44\times37\times54$), a fuselage block ($190\times41\times30$: O-O type), a collar block ($146\times26\times26$: O-H type), a wing block ($143\times43\times34$: O-H type), and a tipcap block ($103\times43\times42$: C-type). The total number of mesh point is about 1.22 million. The collar block is positioned at the interface of wing and fuselage, and a tipcap block on the wing tip to maintain a high-quality mesh. The free stream Mach number is 0.75, and the angle of attack is zero. Numerical techniques for flow analysis are the same as the case of the ONERA-M6 wing.

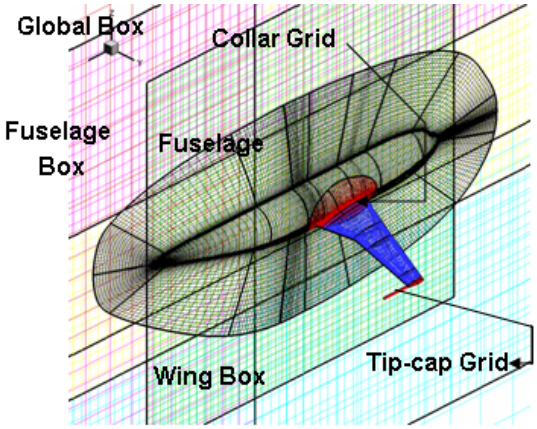

Figure 16. Overset grid system for DLR-F4.

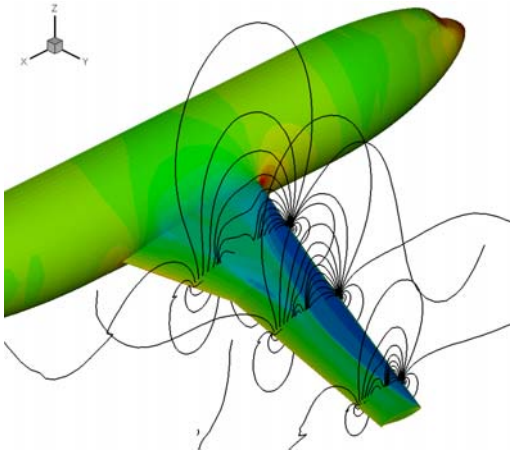

Figure 17. Pressure contour of baseline model.

B. The 1st Stage Design of DLR-F4: Planform Design

The objective function of planform design is the drag coefficient, and lift constraint is imposed as in the case of the ONERA-M6 design. Wing weight during the design process is imposed not to exceed the baseline wing weight as given in Eq. (11). Table 5 presents the comparison of the baseline and the designed geometries through RSM and Kriging model. Unlike the case of the ONERA-M6 wing, values of design variables changes visibly depending on meta-modeling techniques. This may be caused by additional design variables introduced at planform design stage, which make the design space more complex. As shown in Table 6, deviations of the predicted values from the real values are more visible in the case of RSM. Even if RSM has more error and the constraints are not satisfied, discrepancy between the predicted values and the real values are very small (0.6%~2%). In addition, the designed model from RSM yields a better performance. On the other hand, Kriging method predicts the design space more

accurately, and satisfies the design constraint adequately. However, performance improvement is less impressive than the RSM result, because design process is tightly limited by the weight constraint. Figures 18 and 20 show the design planform and the baseline model. Figures 19 and 21 present the comparison of pressure contours of baseline and designed models at each design stage. As in the case of the ONEAR-M6 wing, shock wave on the wing upper surface does not decreases remarkably.

$$\begin{aligned} &Minimize: C_D \\ &Subject\ to: C_L \geq C_{L_0}, C_{L_0} = (Lift\ coefficient\ of\ Baseline\ Model) \\ &W_{W_0} \geq W_W, W_{W_0} = (Wing\ weight\ of\ Baseline\ Model) \end{aligned} \tag{11}$$

Design variable(Dv)		Min	Baseline	Max	Opt. RSM	Opt. Kriging
Dv1	**Sweepback Angle** (Λ)	25°	27.15°	30°	29.863639	27.187492
Dv2	**Kink-Span(S_{kink})**	3733.5	4148.6	4563.2	4102.2392	3886.7324
Dv3	**Semi-Span(S_{semi})**	11682.0	12980.5	14273.0	13067.278	12840.069
Dv4	**Kink-Chord(C_{kink})**	2731.2	3034.7	3338.1	2885.9802	3138.7873
Dv5	**Tip-Chord(C_{semi})**	1401.0	1556.7	1712.4	1660.0990	1570.0544
Dv6	**Twist Angle** (θ)	-5.0°	-4.631°	-3.0°	-4.997680°	-4.445511°
Const.	**Wing Weight(W_{W_0})**		19.9633		20.356594	19.77818

Table 5. Design variables and optimum values of DLR-F4 wing/body.

Obj. fn. & Constraint	Baseline model	RSM		Kriging	
		Predicted value	Real value	Predicted value	Real value
C_L	0.710176	0.710176	0.7058313	0.71020	0.708225
C_D	0.022014	0.019047	0.0204689	0.02139	0.021064
Weight	19.9633	19.96329	20.35259	19.96199	19.77818

Table 6. Comparison of objective functions/constraint values for designed model (planform design/DLR-F4).

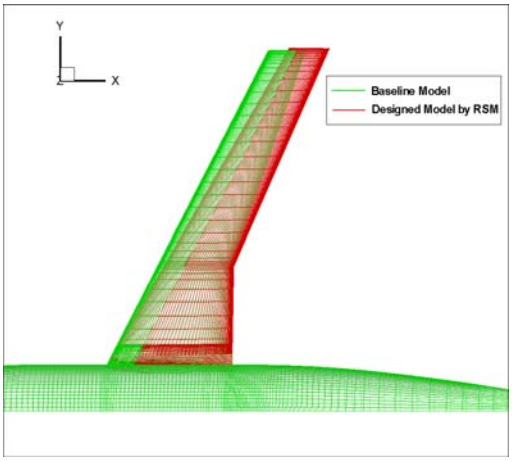

Figure 18. Comparison of baseline model with optimized model by RSM method.

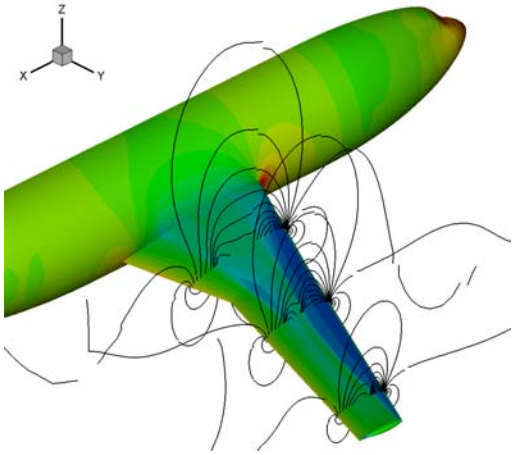

Figure 19. Pressure contour of 1st-stage design model. : RSM+GA

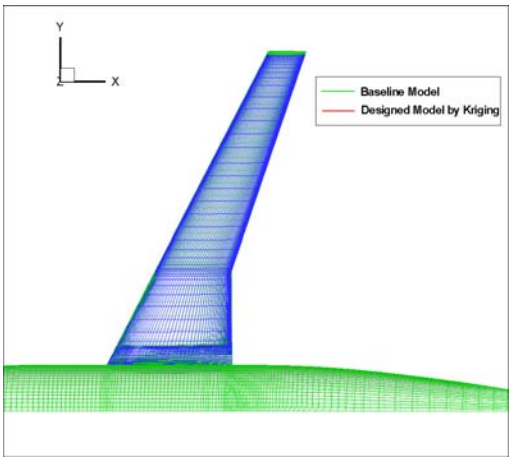

Figure 20. Comparison of baseline model with optimized model by Kriging method.

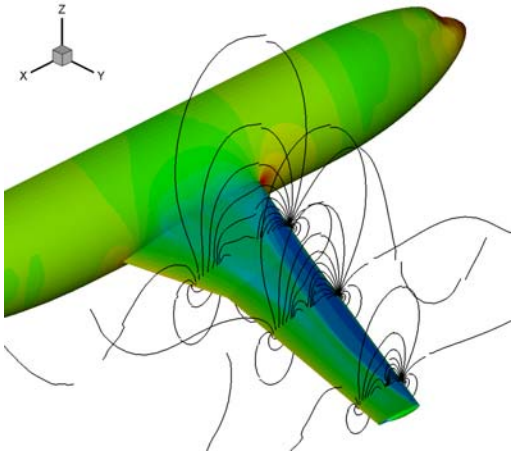

Figure 21. Pressure contour of 1st-stage design model. : Kriging+GA

C. The 2nd Stage Design of DLR-F4: Surface Design

GBOM based on overset discrete adjoint approach is applied to the designed configuration at the 1st stage. The formulation is given by Eq. (12). Wing weight constraint is not considered in this stage, because variation of wing surface design variables is too small to affect the structural safety of the wing. Wing planform designed by RSM and GA is used as the initial geometry for surface design.

$$\begin{aligned} &Minimize: C_D \\ &Subject\ to: C_L \geq C_{L_0}, C_{L_0} = (Lift\ coefficient\ of\ Baseline\ Model) \\ &(Objective\ function) = C_D + Wt \times \left[0, C_{L_0} - C_L\right],\ \ Wt = \frac{\partial C_D}{\partial \alpha} \Big/ \frac{\partial C_L}{\partial \alpha} \end{aligned} \tag{12}$$

Table 7 and Figure 22 show that drag coefficient decreases by 14.08%, and variation of lift coefficient during the design process is less than 1.5% of the initial value. As a result, *L/D* increases from 32.26 to 36.258 after the 2-stage design process. It may look like that the present design improvement is less impressive compared to typical transonic wing case. However, the drag, which is caused by the fuselage, remains at a constant value through the whole design process, because design variables are applied to the wing section only. Thus, the portion of fuselage drag actually increases as the whole drag coefficient decreases at each design step. If effects of the fuselage are considered in actual design process, aerodynamic performance could be more improved than the present result. It is observed that shock strength on wing surface is almost eliminated after the 2-stage design process as shown in Figs. 23-25.

Obj. fn. & Constraint	Baseline model	1st– stage design		2nd-stage design
		RSM + GA	Kriging + GA	RSM + Adjoint
C_L	0.710176	0.7058313	0.708225	0.699597
C_D	0.022014	0.0204686	0.021064	0.019295

Table 7. Comparison of objective functions/constraint values for designed models. (DLR-F4)

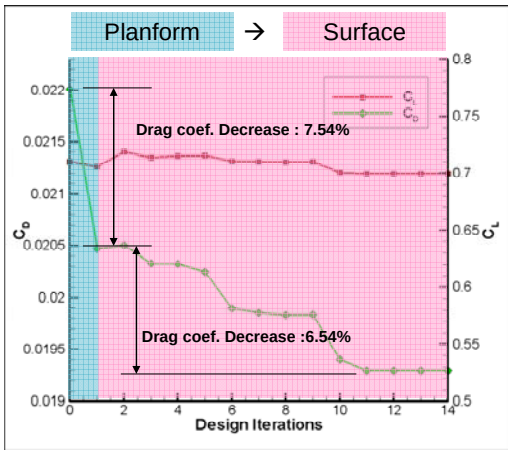

Figure 22. 2-stage design history of DLR-F4.

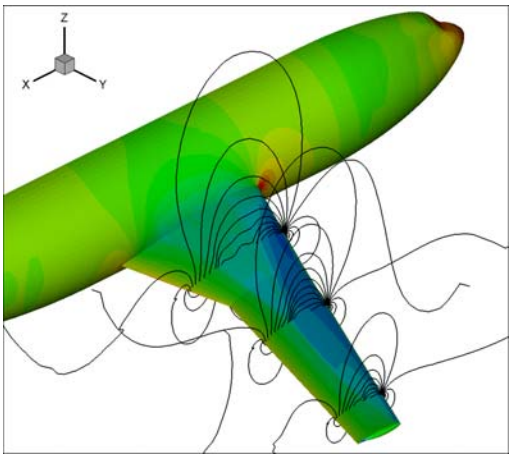

Figure 23. Pressure contour of 2nd-stage designed model.

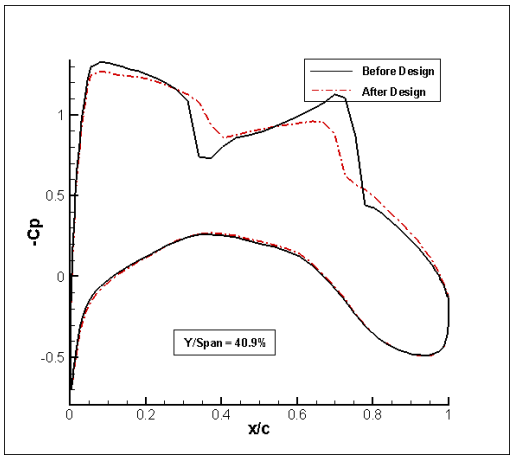

Figure 24. Surface pressure distribution.

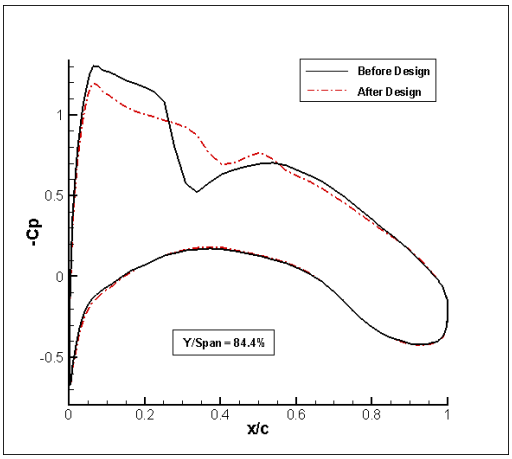

Figure 25. Surface pressure distribution.

V. Conclusion

An efficient high-fidelity multi-stage design optimization approach is proposed by combining global and local optimization techniques. At global optimization stage, design of wing planform is carried out by GA optimizer based on the meta-modeling techniques such as the RSM or Kriging method. At local optimization stage, wing surface is then modified by GBOM approach based on discrete adjoint method which brings a substantial reduction of wave drag. Performance improvements of the designed model are evaluated through the drag decomposition technique. The portion of induced drag and entropy drag analyzed by drag decomposition can provide information on dominant design parameters for drag reduction. The proposed design approach is applied to the re-design of the ONERA-M6 wing and DLR-F4 wing/body configuration. Results of two design cases demonstrate that the proposed multi-stage design approach can improve the aerodynamic performance of three-dimensional aircraft configuration efficiently by exploiting advantages of the global and local optimization methods.

Acknowledgments

The authors appreciate financial supports by 'the Brain Korea-21 Project for the Mechanical and Aerospace Engineering Research at Seoul National University' and 'the Smart UAV Development Program of the 21st Century Frontier R&D Program sponsored by the Ministry of Commerce, Industry and Energy'. The authors are also grateful to 'AFI (Advanced Fluid Information Research Center) of Tohoku University' for the sponsorship of super-computing resources.

References

Periodicals

[1]Sung-soo Kim, Chongam Kim, Oh-hyun Rho, and Seung Kyu Hong, "Cures for the Shock Instability: Development of Shock-Stable Roe Scheme," *Journal of Computational Physics*, Vol. 182, No. 2, 2003, pp. 342-374.

Books

[2]R.H. Myers, and D.C. Montgomery, *Response surface methodology: process and product optimization using design experiments*, Wiley, New York, 1978.

Electronic Publications

[3]John McCall, "Genetic algorithm for modeling and optimization," *Journal of Computational and Mathematics*, Vol. 184, 2005.

[4]H.S Chung and J.J Alonso, "Multiobjective Optimization using Approximation Model-Based Genetic Algorithm", 10th AIAA/ISSMO, Multidisciplinary Analysis and Optimization Conference, AIAA 2004-4325 Albany, NY, September 2004.

[5]Wataru YAMAZAKI, Kisa MATSUSHIMA and Kazuhiro NAKAHASHI, "Aerodynamic Shape Optimization Based on Drag Decomposition," 24th Applied Aerodynamics Conference, AIAA-2006-3332, 2006.

[6]Ahn.J.K., Kim.H.J., Lee.D.H. and Rho.O.H., "Response Surface Method for Aircraft Design in Transonic Flow," Journal of Aircraft, Vol. 38, No.2, pp.231-238.2001.

[7]Jerome Sacks, William J. Welch, Toby J. Mitchell and Henry P. Wynn, "Design and Analysis of Computer Experiments," Statistical Science, Vol. 4, No. 4, pp. 409-435, 1989.

[8]Timothy W. Simpson, Timothy M. Mauery, John J. Korte and Farrokh Mistree, "Comparison of response surface and kriging models for multidisciplinary design optimization," American Institute of Aeronautics and Astronautics, AIAA-98-4755, 1998.

[9]Kasidit Leoviriyakit, Antony Jameson, "Multi-point Wing Planform Optimization via Control Theory," 43rd Aerospace Science Meeting and Exhibit, 2005-0450, January 10-13,Reno, Nevada, 2005.

[10]B.J.Lee and Chongam Kim, "Viscous Aerodynamic Shape Optimization of Wing/Body Configuration with Overset Mesh Techniques," Infotech@Aerospace 2007 Conference and Exhibit, Invited Session (Design Exploration for Aerospace Systems), AIAA-2007-2872, Rohnert Park, California, 7-10 May, 2007

[10]Dimitri J.arvrisplis, "Discrete Adjoint-Based Approach for Optimization Problems on Three-Dimensional Unstructured Meshes," AIAA Journal, Vol. 45, No. 4, April, 2007

[11]W. Liao and H.M. Tsai, "Aerodynamic Design Optimization by the Adjoint Equation Method on Overset Grids," 44th AIAA Aerospace Science Meeting and Exhibit, 2006-54, January 9-12,Reno, Nevada, 2006

[12]E.J Nielsen and W.K Anderson, "Recent Improvements in Aerodynamic Design Optimization on Unstructured Meshes," AIAA Journal, Vol. 40, No. 6, pp. 1155-1163, 2002

[13]S. Koc, H. Kim and K. Nakahashi, "Aerodynamic Design Optimization of Wing-Body Configuration," AIAA paper, 2005-331

[14]R.M. Cumming, M.B. Giles and G.N. Shrinivas, "Analysis of the Elements of Drag in Three-Dimensional Viscous and Invicid Flow," AIAA paper 96-2482-CP, 1996

[15]Micheal B. Giles and Russell M. Cummings, "Wake Integration for Three-Dimensional Flowfield Computation: Theoretical Development," Journal of Aircraft, Vol. 36, No. 2, pp.357-365. 1999

[16]Luigi Paparone and Renato Tognaccini, "Computational Fluid Dynamics-Based Drag Prediction and Decomposition," Journal of Aircraft, Vol. 41, No. 9, pp.1647-1657. 2003

[17]C.P. van Dam, "Recent experience with different methods of drag prediction," Progress in Aerospace Science 35 (1999), pp. 751-798. 1996